

Spectral fluctuations and $1/f$ noise in the order-chaos transition regime

M. S. Santhanam and Jayendra N. Bandyopadhyay

Physical Research Laboratory, Navrangpura, Ahmedabad 380 009, India.

(Dated: May 23, 2019)

Level fluctuations in quantum system have been used to characterize quantum chaos using random matrix models. Recently it was shown, using time series analogy, that level fluctuations inherently carry signatures of the underlying classical dynamics in the regular and chaotic limit. We show that quite generally the spectral transition accompanying regularity to chaotic dynamics displays characteristic $f^{-\gamma}$ noise, with $1 \leq \gamma \leq 2$. We demonstrate this using a smooth potential and a kicked system modeled by Gaussian and circular ensembles respectively of random matrix theory. We also discuss the effect of short periodic orbits on these fluctuation measures.

PACS numbers: 05.45.Mt, 05.40.-a, 05.45.Pq, 05.40.Ca

I. INTRODUCTION

Quantum chaos, the study of quantum analogues of classically chaotic systems, is characterized by the fluctuation properties of the spectrum of its Hamiltonian operator. As shown by Berry and Tabor, for quantum systems with regular classical dynamics, the spectral fluctuations are Poisson distributed [1]. This corresponds to the tendency of the eigenvalues to cluster together. On the other hand, one of the remarkable results established by Bohigas *et al* is that the level fluctuation properties of quantum systems, whose classical limit is chaotic, are identical to those of an appropriate ensemble from random matrix theory (RMT) [2]. This is the level repulsion regime, i.e., the eigenvalues tend to repel one another. From a semiclassical point of view, this corresponds to long time behavior of the classical periodic orbits. Thus, in this sense, characterizing quantum chaos in terms of presence or absence of level repulsion requires invoking the spectral properties of random matrix ensembles. Recently, in analogy with time series, a method has been proposed to characterize spectral fluctuations using inherent properties of the spectrum [3]. If the eigenvalues of Hamiltonian operators could be thought of as a time series, and the eigenvalue index would then correspond to time in some units, then the methods of traditional time series analysis can be applied to it. Thus, it has been shown that the power spectrum $\langle S(f) \rangle$ of the fluctuations in the cumulative level density averaged over several realizations that constitute the ensemble, displays $1/f$ or $1/f^2$ behavior depending on whether the system is classically chaotic or classically regular [4]. A theoretical justification of this phenomenon has been given based on random matrix theory [4]. Level sequences from an ensemble of random matrices were analyzed in this framework and shown to have power spectrum that is characterized by $1/f$ or $1/f^2$ noise, depending on the degree of level repulsion. This work also showed examples of atomic level sequences displaying $1/f$ noise. Thus, atomic levels join the host of other systems and phenomena that display $1/f$ noise leading to the well known cliché that $1/f$ is ubiquitous in nature [5].

In this paper, we focus on the systems whose classical

dynamics displays mixed phase space, i.e., both regular and irregular motion coexist, to study the transition region between regularity and chaos. As we vary a parameter, the system would make a smooth transition from regular to predominantly chaotic dynamics. Such systems are generic rather than exceptions. For instance, the entire class of atoms in strong fields problems, range of problems involving atoms in time-varying fields, modeled by δ -kicked potentials, are all mixed phase space systems. In this work we consider two models that are paradigms of quantum chaos for dynamics in a smooth potential and kicked systems, namely the coupled quartic oscillators and the kicked top. In both these cases, by varying a single parameter, we observe a transition in the qualitative dynamics of the system and they have been extensively studied before. Thus, as opposed to real atomic systems, we can control the degree of classical chaos in these models. In particular, we explore the transition region using the power spectrum of the spectral fluctuations. Based on the numerical evidence, we show that, in general, the power spectrum goes as, $\langle S(f) \rangle \propto f^{-\gamma}$, where $1 \leq \gamma \leq 2$.

From the RMT point of view, these model systems possess symmetries (time-reversal invariance without spin-1/2 interactions) that put them in a class of matrices described by the orthogonal ensemble of RMT [6]. For kicked systems, the eigenvalues of the Floquet operator are unimodular and are part of the circular orthogonal ensemble (COE) whereas the oscillator system falls in the Gaussian orthogonal ensemble (GOE) class. We also point out that kicked top resides in finite dimensional Hilbert space in contrast to the quartic oscillator that resides in infinite dimensional Hilbert space. Thus, the results reported here also illustrate the applicability of ‘time series analogy’ to kicked systems and circular ensembles. In the random matrix literature, the regular to chaos transition region is described by phenomenological formulas that smoothly interpolate between, say, Poisson to GOE distribution. We apply one such distribution introduced by Izrailev [8] whose single parameter $\beta = 0$ gives a Poissonian form and approximates GOE closely in the limit $\beta = 1$. We show that the exponent of the power spectrum γ correlates strongly with β . This estab-

lishes that γ reflects the underlying changes in the nature of classical dynamics.

In semiclassical systems of the type we consider in this work, periodic orbits via the Gutzwiller formalism play an important role in determining the quantum spectrum. As established by the work of Berry [9], the properties of the spectrum on a scale of mean level spacing are determined by very long time period orbits and in a sense both of them display universality; the RMT type universality in the spectrum and classical universality embodied in the Hannay-Ozorio sum rule [10]. However, long range spectral properties are determined by the short time periodic orbits which are system specific and are not universal. This manifests itself in the power spectrum as deviations from the $f^{-\gamma}$ behavior of the cumulative density fluctuations that we study in this work. We show the effect of short time periodic orbits in the quartic oscillator system, where scarring or the density enhancements in the vicinity of certain periodic orbits [11] is a prominent feature due to these orbits.

In recent years, several studies show that RMT has a larger domain of application far beyond its original putative domain, namely, the nuclear physics. Random matrix theory was originally proposed as a means to understand spectrum of high dimensional, complex quantum systems such as those of nucleus or atomic systems, whose detailed description continues to be a challenge even today. In fact, the range of studies show that it extends beyond the traditional quantum physics as one can see from its applications in such apparently disparate fields ranging from number theory to econophysics, multivariate statistics to condensed matter physics and quantum chromodynamics [12]. It is now well known that RMT describes spectral fluctuations of empirical cross-correlation matrices [13]. In this approach, the spectrum of the correlation matrices drawn from multivariate time series is treated as though it is drawn from a Hamiltonian system. The idea that eigenvalues could be thought of as a time series complements this earlier stream of work.

We describe our models in Sec.II and the basic tools in Sec.III and present our results in subsequent sections.

II. MODELS

A. Coupled quartic oscillator

The Hamiltonian for the coupled quartic oscillator is,

$$H_1 = p_1^2 + p_2^2 + q_1^4 + q_2^4 + \alpha q_1^2 q_2^2. \quad (1)$$

This system is classically integrable for $\alpha = 0, 2, 6$ and the phase space is predominantly chaotic for $\alpha > 6$. This has been extensively studied as a model for chaotic dynamics in a smooth potential [14, 15]. To study the quantum analogue of this oscillator, we solve the corresponding Schrödinger equation in the unperturbed basis, i.e., the basis of the eigenfunctions corresponding to $\alpha = 0$. Thus,

the matrix elements of Hamiltonian operator \hat{H}_1 is computed in the chosen basis and a sufficiently large Hamiltonian matrix is diagonalized to obtain its eigenvalues. In this work, we diagonalize a matrix of order about 13000 to obtain about 2000 eigenvalues converged to at least 8 digits. This system possesses C_{4v} point group symmetry, i.e., all the invariant transforms of a square. We symmetry decompose our quantum spectra and study the levels from only the A_1 irreducible representation.

B. Quantum Kicked Tops

The quantum top [16] is characterized by an angular momentum vector \mathbf{J} , whose components (J_x, J_y, J_z) obey usual commutation relations and the dynamics is such that \mathbf{J}^2 is conserved. The dynamics of the top is governed by the Hamiltonian [16],

$$H_2(t) = \frac{\pi}{2} J_y + \frac{k}{2j} J_z^2 \sum_{n=-\infty}^{\infty} \delta(t-n). \quad (2)$$

The first term describes the precession around the y axis with angular frequency $\pi/2$ and the second term kicks in periodically with δ -function kicks of strength k . Each kick can be thought of as an impulsive rotation about z -axis by an angle proportional to J_z and the proportionality constant is $k/2j$.

The unitary time evolution operator, which transports an initial state through a precession and a subsequent kick, is given by,

$$U = \exp\left(-i\frac{k}{2j}J_z^2\right) \exp\left(-i\frac{\pi}{2}J_y\right). \quad (3)$$

In this work, the power spectrum is taken using the eigenvalues of this operator. In the limit $j \rightarrow \infty$, we can derive a classical map whose dynamics is controlled by the parameter k . We do not show the map here as it has been extensively studied in Refs. [16]. For our purposes, we note that for $k = 1$, the classical map is nearly regular. For $k > 1$, the dynamics becomes increasingly chaotic. At $k = 6$, only minuscule islands are visible in the phase space [17].

III. SPECTRAL FLUCTUATIONS

We denote the eigenvalues of the appropriate operator described above by E_i , $i = 1, 2, \dots, n + 1$. The level density is,

$$\rho(E) = \sum \delta(E - E_i) \equiv \bar{\rho}(E) + \rho_{osc}(E) \quad (4)$$

where $\bar{\rho}(E)$ and $\rho_{osc}(E)$ denote the average and the oscillatory part. In a similar vein, we can define the spectral counting function or the integrated level density as, $N(E) = \bar{N}(E) + N_{osc}(E) = \int^E \rho(E') dE'$. In order to

compare the spectral fluctuations from various systems it is customary to unfold the spectrum by a transformation $\lambda_i = \overline{N}(E_i)$, such that the mean level density of the transformed levels $\overline{\rho}(\lambda) = 1$. All further analysis is carried out using the sequence $\{\lambda\}$. For instance, the nearest neighbor spacing is given by,

$$s_i = \lambda_{i+1} - \lambda_i \quad i = 1, 2, \dots, n. \quad (5)$$

The distribution of spacings probes the short range correlations in the spectrum and RMT predicts spacing distribution to be,

$$P(s) = \frac{\pi s}{2} \exp\left(-\frac{\pi s^2}{4}\right) \quad (6)$$

for the GOE case. In this paper, we will work with the statistics given by,

$$\delta_n = \sum_{i=1}^n (s_i - \langle s \rangle) = -N_{osc}(E). \quad (7)$$

Once unfolding is performed, on an average, a unit interval of the spectrum will have one level. Hence, δ_n represents the cumulative deviation until n th level, of the i th unfolded level from i . This quantity has a formal analogy with a time series. If the index i represents the (scaled) time, then $(s_i - \langle s \rangle)$ represents the actual value assumed by the series at the i th time instant. However, note that since negative spacings are not allowed, $(s_i - \langle s \rangle) > -1$, which need not be true for a real time series data [4]. Following Ref [3], we take the power spectrum of δ_n defined by,

$$S(\tau) = |\widehat{\delta}_\tau|^2 = \left| \frac{1}{\sqrt{n+1}} \sum_k \delta_k \exp\left(\frac{-2\pi i \tau k}{n+1}\right) \right|^2 \quad (8)$$

where $\tau = 1, 2, \dots, n$; $\widehat{\delta}_\tau$ is the Fourier transform of δ_n . In a sense, $\widehat{\delta}_\tau$ is the integrated density counterpart of the spectral form factor that is widely studied in semiclassics and random matrix literature [6]. From RMT considerations, it is shown in Ref. [4] that,

$$\begin{aligned} \langle S(\tau) \rangle &\propto \tau^{-2} & \text{GDE} \\ &\propto \tau^{-1} & \text{GOE, GUE, GSE} \end{aligned} \quad (9)$$

where $\langle \cdot \rangle$ represents the ensemble average. In this, GDE is the so-called Gaussian diagonal ensemble, an appropriate one for regular systems. Here GUE and GSE represent Gaussian unitary and symplectic ensemble respectively. The power spectrum goes as $1/\tau$ for all the Gaussian ensembles (other than GDE) that are appropriate for chaotic limit in the sense of Bohigas *et al* [2]. In the next sections, we will present results to infer that

$$\langle S(\tau) \rangle \propto \tau^{-\gamma} \quad 1 \leq \gamma \leq 2 \quad (10)$$

and the value of γ depends on the degree of chaos in the system.

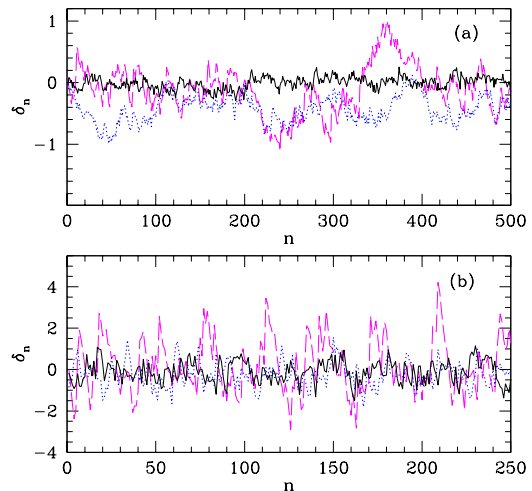


FIG. 1: (Color online) $\delta_n - n$ curve for (a) kicked top and (b) quartic oscillator. The solid curve corresponds to chaotic limit ($k = 7, \alpha = 20$) and the dotted curve corresponds to intermediate region ($k = 3, \alpha = 12$). The dashed curve corresponds to regular limit ($k = 1, \alpha = 0$).

Before we plunge into the results, we show the statistics δ_n for our models described in the previous section. In the case of quartic oscillator given in Eq.(1), using the result in Ref. [18], we obtain, in the asymptotic limit, the smooth part of the integrated level density to be ($\hbar = 1$),

$$\overline{N}(E) = \frac{E^{3/2}}{6} F\left(\frac{1}{2}, \frac{1}{2}; 1; \frac{2-\alpha}{4}\right) \quad (11)$$

where $F(\cdot)$ is the Gauss' Hypergeometric function [19]. However, this relation does not hold good if we source our levels from A_1 irreducible representation of C_{4v} group, as we have done in this paper. Then, we symmetry decompose this level density. Performing the symmetry decomposition using the method in Ref. [20], we obtain the approximate integrated level density for the A_1 representation,

$$\begin{aligned} \overline{N}_{A_1}(E) = \frac{1}{8} &\left[\overline{N}(E) + \frac{\Gamma(5/4)E^{3/4}}{\Gamma(7/4)\sqrt{\pi}2^{7/4}} \right. \\ &\left. + \frac{E^{3/4}}{\Gamma(7/4)\sqrt{2\pi}(2+\alpha)} + \frac{3}{4} \right]. \end{aligned} \quad (12)$$

Note that the symmetry decomposition has provided additional nontrivial contributions of $O(E^{3/4})$. We use this expression to unfold the quartic oscillator levels.

In Fig. 1 we show the plots of $\delta_n - n$ for the quartic oscillator and the kicked top for a choice of 3 parameters in the regular, chaotic and the transition region. In Fig. 1(a) for the kicked top, the dashed curve corresponding to the Poisson spectrum ($k = 1$) differs markedly from the solid curve corresponding to the linear level repulsion ($k = 7$) limit. We also plot an intermediate case (dotted

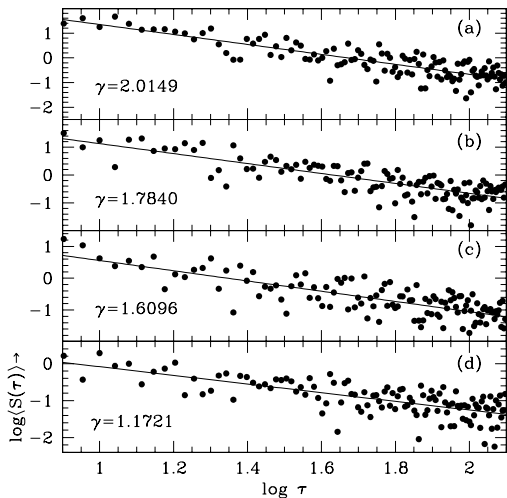


FIG. 2: Power spectrum of δ_n for kicked top at (a) $k = 1$, (b) $k = 2.0$, (c) $k = 3.0$ and (d) $k = 7.0$. The solid line is the least squares fit. The slope γ is indicated in each graph.

curve) to show the transition taking place from Poisson to GOE type spectrum. The intermediate case at $k = 3$ also differs from the other two and is qualitatively different. We observe similar features for the quartic oscillator in Fig. 1(b) for $\alpha = 6, 11.5, 19.5$, as also reported in an earlier work of Bohigas [21].

IV. POWER SPECTRUM IN TRANSITION REGION

In Figs. 2 and 3, we display the ensemble averaged power spectrum of δ_n in log scale. Ensemble averaging is done as follows : in the case of quartic oscillator, for each value of α , we obtain 2000 converged levels. After leaving out the first 200 levels, we create 3 sequences of 600 levels each. We further obtain similar sequences from more values of α separated by $\delta\alpha = 0.1$. For instance, in Fig. 3(b), we show results for $\alpha = 11.5$, which corresponds to ensemble average in the range $\alpha = 11.2 - 11.8$ in steps of 0.1. Thus, the results (except for the integrable case in Fig. 3(a)) represent an average over 21 level sequences of length 600 each. For the integrable case, the ensemble consists 9 level sequences (3 from each of $\alpha = 0, 2$ and 6) of length 600 each. Similar ensemble averaging is performed for the kicked top with 11 level sequences of length 800 each.

For the case of regular and chaotic limit shown in Figs. 2(a,d) and 3(a,d), there is a fairly good agreement with the predicted slopes in Eq.(9). There are deviations for $\tau < \tau_{\min}$, due to the effect of short periodic orbits with scaled time period τ_{\min} . The deviation for large τ arises from approaching the Nyquist frequency, $\tau = (n + 1)/2$. It is clear from Figs. 2,3(b,c) that as the system explores the region intermediate between the regular and

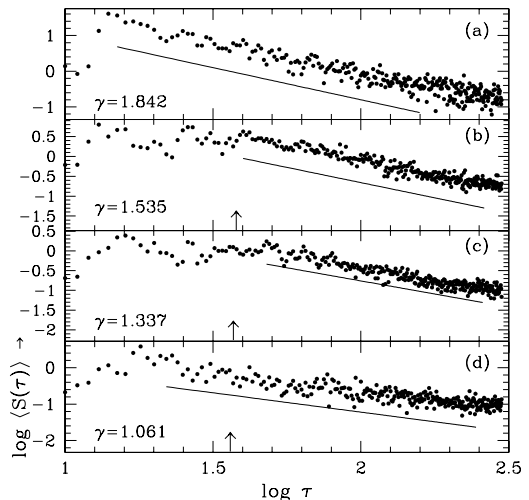


FIG. 3: Power spectrum of δ_n for quartic oscillator at (a) $\alpha=0,2,6$ (b) $\alpha=7.5$ (c) $\alpha=11.5$ and (d) $\alpha=19.5$. The solid lines are the least squares fit with intercept shifted for clarity. The slope γ is indicated in each graph. The arrows in (b-d) indicates the value of $\log \tau_{\min}$ corresponding to the time period of the short periodic orbit. The linearity in the power spectrum is expected to hold for $\tau > \tau_{\min}$.

the chaotic limit, the slope γ takes on values between 1 and 2. This is demonstrated in both the quartic oscillator and the kicked top.

In order to obtain a global picture, we compute the power spectrum for a range of parameter values in the order-chaos transition region of the oscillator and the top. As pointed out earlier, in RMT literature the transition from regular to chaotic dynamics is parameterized by a single parameter family for spacing distribution $P(s)$, which goes from being Poisson to GOE as a free parameter in the distribution, say β , is varied from 0 to 1. The commonly used one is the Brody distribution [7]. In this paper, we use the distribution P_T introduced by Izrailev [8] which is more accurate than the Brody distribution :

$$P_T(s) = A s^\beta (1 + B \beta s)^{f(\beta)} \exp \left[\frac{-\beta \pi^2 s^2}{16} - \frac{\pi s}{2} \left(1 - \frac{\beta}{2} \right) \right] \quad (13)$$

where A and B are normalizing parameters and $f(\beta) = 2^\beta (1 - \beta/2)/\beta - 0.16874$. For $\beta = 0$, this distribution gives a Poissonian form and for $\beta = 1$ it closely approximates GOE spacing distribution, which is our region of interest in this work. The intermediate values of β between 0 and unity corresponds to transition statistics. The Fig. 4 shows that the series of β and γ display similar trend and are strongly correlated for both the top and the oscillator. Hence we infer that the scaling exponent γ of the power spectrum reflects the underlying qualitative trends in the nature of classical dynamics of the system. In addition to the Poisson and GOE limits, it also captures the intermediate statistics. Thus, in gen-

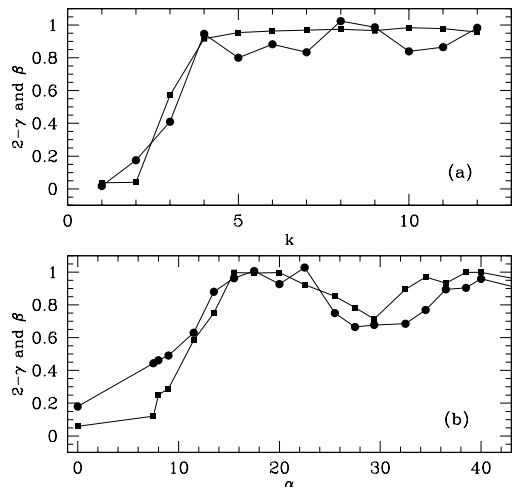


FIG. 4: The parameter β (squares) in $P_T(s)$ as a function of chaos parameter for (a) the kicked top and (b) quartic oscillator. Also plotted is the shifted slope $2 - \gamma$ (circles) of the power spectrum in Eq.(10). The slope is shifted such that y -axis lies in the range 0 to 1. This figure shows that β is strongly correlated with γ .

eral, the power spectrum of δ_n goes as, $\langle S(\tau) \rangle \propto \tau^{-\gamma}$, where $1 \leq \gamma \leq 2$ for Poisson to GOE transitions. The distribution $P_T(s)$ has limits $\beta = 2, 4$ corresponding to GUE and GSE spacing distributions respectively. We expect that similar behavior as reported in Fig. 4 would be observed for systems in GUE and GSE class.

V. EFFECT OF SHORT PERIODIC ORBITS

As opposed to purely random matrices, the semiclassical systems show deviations from results given by Eq.(9) for $\tau < \tau_{\min}$, where τ_{\min} is the period t_{\min} of the shortest periodic orbit scaled with respect to the Heisenberg time (τ_H), $\tau_{\min} = t_{\min}/2\pi\hbar\bar{\rho}$. Physically this corresponds to short periodic orbits being system specific features and in the corresponding large energy scales universality breaks down leading to deviations from RMT based results. This has been brought out in the remarkable results due to Berry [9]. Thus, the validity of power spectrum scaling is restricted to $\tau_{\min} \ll \tau \ll \tau_H$. The short period orbit in the quartic oscillator is the ‘channel orbit’, as it is referred to in the literature, with the initial condition $(q_1 = 0, q_2, p_1 = 0, p_2)$. This can be identified by taking discrete Fourier transform of the scaled energies of the oscillator [21, 22]. The time period of this orbit is

$$T(E) = E^{-1/4} \sqrt{\pi} \frac{\Gamma(1/4)}{2\Gamma(3/4)}. \quad (14)$$

Using this relation we obtain, among all the sequence of levels that form the ensemble, the period of the short period orbits and have indicated it in Fig. 3. This provides

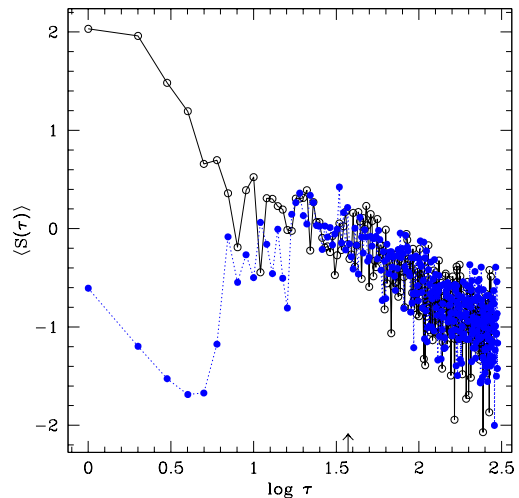


FIG. 5: (Color online) The effect of short periodic orbits in the spectrum. The power spectrum for quartic oscillator with $\alpha = 30$ including the levels containing localized states (dotted). The arrow indicates the value of τ_{\min} . The solid line is the power spectrum after localized states are removed. See text for details.

the lower bound to the region of validity for power law scaling in the power spectrum $\langle S(\tau) \rangle$.

In Fig. 5, we show the effect of short periodic orbits on the power spectrum of δ_n . First note that for the quartic oscillator at $\alpha = 20$, $\gamma = 1.073$ whereas for $\alpha = 30$ we have $\gamma = 1.322$. The β parameter also shows a similar trend. In general, we would expect that as α increases monotonically, chaos also increases and hence agreement with RMT should get better. But numbers quoted above show that, roughly speaking, chaos at $\alpha = 20$ is more than at $\alpha = 30$. This ‘anomalous’ feature is the effect of oscillating stability of the short periodic orbits. At $\alpha = 20, 30$ the short periodic orbit undergoes an anti-pitchfork and a pitchfork bifurcation respectively. This, in turn, affects the spectral levels. It is known that the short periodic orbits influence a series of eigenstates in the quartic oscillator spectrum [15, 23]. This series of states is referred to as the localized or sometimes scarred states and is characterized by strong deviations from RMT for eigenvector statistics [24]. These states can also be treated analytically within the framework of adiabatic theory [15, 23]. If we remove the eigenvalues corresponding to these localized states in the spectrum and then take the spacing distribution, then we might expect a better agreement with RMT. This is like removing the effect of short periodic orbits in the spectrum. The dotted line in Fig. 5 is for the spectrum with localized states included and the solid line corresponds to the spectrum with localized states removed. In this example, the ensemble has just 3 level sequences of 600 levels each which is reflected in large amplitude of fluctuations. The power spectrum changes character for $\tau < \tau_{\min}$ and the range of validity

of linear scaling in the power spectrum gets better. This is a manifestation of the effect of short periodic orbits in the spectrum.

VI. CONCLUSIONS

In summary, we have shown that the fluctuations in the energy spectra of quantum systems display $f^{-\gamma}$ noise, where the particular value assumed by γ within the limits $1 \leq \gamma \leq 2$ reflects the underlying nature of classical dynamics, namely, regular or chaotic or a mixture thereof. We also demonstrate that this result holds good for smooth potentials (modeled by Gaussian ensembles

of RMT) and also for the kicked systems (modeled by the circular ensembles). Earlier, it was shown that the quantum spectrum of a classically regular system displays $1/f^2$ noise and chaotic case displays $1/f$ noise. This work lends credence to the result that energy fluctuations can be used to characterize the spectrum and $f^{-\gamma}$ type noise, with $1 \leq \gamma \leq 2$, is an inherent characteristic of quantum systems.

Acknowledgments

We thank Prof. V. B. Sheorey and Dr. Dilip Angom for useful discussions.

-
- [1] M. V. Berry and M. Tabor, *Proc. R. Soc. Lond. A* **356**, 375 (1977).
 - [2] O. Bohigas, M.-J. Giannoni and C. Schmidt, *Phys. Rev. Lett.* **52**, 1 (1984).
 - [3] A. Relaño *et al.*, *Phys. Rev. Lett.* **89**, 244102 (2002); S. N. Evangelou and D. E. Katsanos, *Phys. Lett. A* **334**, 331 (2005).
 - [4] E. Faleiro *et al.*, *Phys. Rev. Lett.* **93**, 244101 (2004).
 - [5] B. Roy Frieden, *Physics from Fisher Information* (Cambridge, UK, 1998); Bruce J. West and M. F. Shlesinger, *American Scientist* **78**, 40 (1990); Edoardo Milotti, physics/0204033 (2002).
 - [6] M. L. Mehta, *Random Matrices* (Academic Press, New York, 1991); F. Haake, *Quantum Signatures of Chaos*, 2nd ed. (Springer-Verlag, Berlin, 2000).
 - [7] T. A. Brody, *Lett. Nuovo Cimento* **7**, 482 (1973).
 - [8] F. M. Izrailev, *Phys. Lett. A* **134**, 13 (1988); *J. Phys. A* **22**, 865 (1989); See in particular G. Casati, F. Izrailev and L. Molinari, *J. Phys. A* **24**, 4755 (1991).
 - [9] M. Berry, *Proc. R. Soc. Lond. A* **422**, 7 (1989).
 - [10] J. H. Hannay and A. M. Ozorio de Almeida, *J. Phys. A* **17**, 3429 (1984).
 - [11] E. Heller, *Phys. Rev. Lett.* **53**, 1515 (1984).
 - [12] T. Guhr, A. Muller-Groeling and H. A. Weidenmuller, *Phys. Rep.* **299**, 189 (1998).
 - [13] L. Laloux *et al.*, *Phys. Rev. Lett.* **83**, 1467 (1999); V. Plerou *et al.*, *Phys. Rev. Lett.* **83**, 1471 (1999); M. S. Santhanam and P. K. Patra, *Phys. Rev. E* **64**, 016102 (2001); M. S. Santhanam and H. Kantz, *Phys. Rev. E* **69**, 056102 (2004).
 - [14] O. Bohigas, S. Tomsovic and D. Ullmo, *Phys. Rep.* **223**, 43 (1993).
 - [15] B. Eckhardt, G. Hose and E. Pollack, *Phys. Rev. A* **39**, 3776 (1989).
 - [16] F. Haake, M. Kús and R. Scharf, *Z. Phys. B - Condensed Matter* **65**, 381 (1987).
 - [17] J. N. Bandyopadhyay and A. Lakshminarayan, *Phys. Rev. E* **69**, 016201 (2004).
 - [18] S. G. Matinyan and Y. Jack Ng, *J. Phys. A* **36**, L417 (2003).
 - [19] M. Abramowitz and I. Stegun, *Handbook of Mathematical Functions* (Dover, New York, 1970).
 - [20] N. D. Whelan *J. Phys. A* **30**, 533 (1997).
 - [21] O. Bohigas in *Chaos and Quantum Physics*, eds. M.-J. Giannoni, A. Voros and J. Zinn-Justin (North-Holland, 1991).
 - [22] H.-J. Stöckmann, *Quantum Chaos* (Cambridge Univ. Press, Cambridge, England, 1999).
 - [23] M. S. Santhanam *et al.*, *Phys. Rev. E* **57**, 345 (1998).
 - [24] M. S. Santhanam, V. B. Sheorey and A. Lakshminarayan, *Pramana* **48**, 439 (1997).